



OPEN ACCESS

EDITED BY

Lichuan Wu,
Uppsala University, Sweden

REVIEWED BY

Wenli Qiao,
Jiangsu Ocean University, China
Hailun He,
Second Institute of Oceanography,
Ministry of Natural Resources, China

*CORRESPONDENCE

Il-Ju Moon
ijmoon@jejunu.ac.kr

[†]These authors have contributed
equally to this work and share
first authorship

SPECIALTY SECTION

This article was submitted to
Physical Oceanography,
a section of the journal
Frontiers in Marine Science

RECEIVED 16 September 2022

ACCEPTED 31 October 2022

PUBLISHED 17 November 2022

CITATION

Lee W, Kim S-H, Moon I-J, Bell MM and Ginis I (2022) New parameterization of air-sea exchange coefficients and its impact on intensity prediction under major tropical cyclones. *Front. Mar. Sci.* 9:1046511. doi: 10.3389/fmars.2022.1046511

COPYRIGHT

© 2022 Lee, Kim, Moon, Bell and Ginis. This is an open-access article distributed under the terms of the Creative Commons Attribution License (CC BY). The use, distribution or reproduction in other forums is permitted, provided the original author(s) and the copyright owner(s) are credited and that the original publication in this journal is cited, in accordance with accepted academic practice. No use, distribution or reproduction is permitted which does not comply with these terms.

New parameterization of air-sea exchange coefficients and its impact on intensity prediction under major tropical cyclones

Woojeong Lee^{1,2†}, Sung-Hun Kim^{3†}, Il-Ju Moon^{2*}, Michael M. Bell⁴ and Isaac Ginis⁵

¹Forecast Research Department, National Institute of Meteorological Sciences, Jeju, South Korea

²Graduate Program in Marine Meteorology/Typhoon Research Center, Jeju National University, Jeju, South Korea, ³Korea Institute of Ocean Science and Technology, Busan, South Korea,

⁴Department of Atmospheric Science, Colorado State University, Fort Collins, CO, United States,

⁵Graduate School of Oceanography, University of Rhode Island, Narragansett, RI, United States

Understanding and quantifying air-sea exchanges of enthalpy and momentum fluxes are crucial for the advanced prediction of tropical cyclone (TC) intensity. Here, we present a new parameterization of air-sea fluxes at extreme wind speeds from 40 m s^{-1} to 75 m s^{-1} , which covers the range of major TCs. Our approach assumes that the TC can reach its maximum potential intensity (MPI) if there are no influences of external forces such as vertical wind shear or other environmental constraints. This method can estimate the ratio of the enthalpy and momentum exchange coefficient (C_k/C_d) under the most intense TCs without direct flux measurements. The estimation showed that C_k/C_d increases with wind speed at extreme winds above 40 m s^{-1} . Two types of surface layer schemes of the Hurricane Weather and Research Forecast (HWRF) were designed based on the wind speed dependency of the C_k/C_d found at high winds: (i) an increase of C_k/C_d based on decreasing C_d ($C_d\text{-DC}$) and (ii) an increase of C_k/C_d based on increasing C_k ($C_k\text{-IC}$). The modified surface layer schemes were compared to the original HWRF scheme (using nearly fixed C_d and C_k at extreme winds; CTRL) through idealized experiments and real-case predictions. The idealized experiments showed that $C_d\text{-DC}$ reduced frictional dissipation in the air-sea interface as well as significantly reduced sea surface cooling, making the TC stronger than other schemes. As a result, $C_d\text{-DC}$ reduced the mean absolute error and negative bias by 15.0% (21.0%) and 19.1% (32.0%), respectively, for all lead times of Hurricane Irma in 2017 (Typhoon Mangkhut in 2018) compared to CTRL. This result suggests that new parameterization of C_k/C_d with decreasing C_d at high winds can help improve TC intensity prediction, which currently suffers from underestimating the intensity of the strongest TCs.

KEYWORDS

air-sea exchange coefficients, lifetime maximum intensity, maximum potential intensity, numerical modeling, tropical cyclone intensity predictions

Introduction

Prediction of the tracks of tropical cyclones (TCs) has significantly improved over the last decades, but there has been less progress in intensity prediction despite the considerable advancement in technologies for TC-related physics, computational power, numerical modeling, and observations during the same period (DeMaria et al., 2014; Soloviev et al., 2014). TC intensity prediction is challenging because the various environmental effects, inner core dynamics, and underlying surface forcings involved in the intensity change are not entirely understood (Elsberry et al., 2013). In particular, the unresolved physics of the momentum and enthalpy transfer between the atmosphere and the ocean at extreme wind speeds are crucial factors that hamper accurate TC intensity prediction (Moon et al., 2004; Moon et al., 2007).

Figure S1 shows the bias of the HWRF in predicting the 10 m maximum wind speed (MWS) for 2016–2020 in the North Atlantic (NA), the eastern North Pacific (ENP) and the western North Pacific (WNP) TCs, on the basis of 82,821 predictions. The HWRF is an atmosphere-ocean coupled model customized for the hurricane or tropical storm application (Biswas et al., 2018); it is a real-time TC forecasting system operational at the National Centers for Environmental Prediction (NCEP) since the 2007 TC season. Overall, a negative bias (underestimation) is evident above 40 m s^{-1} , significantly increasing with MWS (Figure S1). It reaches -20 m s^{-1} for intense TCs with an MWS above 80 m s^{-1} . This significant bias may be partly attributed to the insufficient horizontal grid resolution of the model (Bender and Ginis, 1999). Another possible reason is the inadequate representation of some physical processes, including the air-sea momentum and enthalpy exchanges at high wind speeds.

TC intensity depends strongly on the coefficients of the transfers of momentum (C_d) and enthalpy (C_k) between the ocean and the atmospheric boundary layer (Ooyama, 1969; Rosenthal, 1971; Emanuel, 1986; Bryan, 2012; Green and Zhang, 2013; Green and Zhang, 2014; Zhang and Emanuel, 2016). In particular, the theoretical MWS of a TC depends on the ratio of the enthalpy coefficient to the momentum exchange coefficient— $(C_k/C_d)^{1/2}$ —in the high-wind speed core of the storm (Emanuel, 1986). Estimating the most accurate C_k/C_d and its behavior at high wind speeds is essential for accurate TC intensity prediction (Green and Zhang, 2013; Soloviev et al., 2014).

The perceived importance of the dependence of the TC intensity on the C_k/C_d has led to considerable effort to measure the exchange coefficients at hurricane-strength wind speeds (DeCosmo et al., 1996; Black et al., 2007; French et al., 2007; Zhang et al., 2008; Haus et al., 2010; Bell et al., 2012; Hsu et al., 2019; Curcic and Haus, 2020; Richter et al., 2021). However, these observations deliver less accuracy at high winds. For exchange coefficient estimates based on the mean profile data

obtained from dropsondes in TCs, the accuracies are known to be 50% and 200% for C_d and C_k , respectively (Richter et al., 2016). Likewise, laboratory estimations of C_d and C_k have limitations because conditions of field observations such as wave age, wavelength, spray, and fetch cannot be considered realistically. These limitations make the determination of air-sea exchanges at extreme wind speeds and their wind dependency difficult (Richter et al., 2016).

In this study, we propose an alternative method in which C_k/C_d at very high wind speeds is indirectly estimated by matching the observed lifetime maximum intensity (LMI) of a TC with the theoretical maximum potential intensity (MPI). This method is based on the assumption that the LMI can reach the MPI if there are no negative influences on the maximum achievable intensity (Emanuel, 1995; Bister and Emanuel, 1998). The equation is

$$\text{MPI}^2 = \frac{C_k}{C_d} \frac{T_{\text{sea}} - T_o}{T_o} (k^* - k) \approx \text{LMI}^2 \quad (1)$$

$$\frac{C_k}{C_d} = \text{LMI}^2 \left(\frac{T_{\text{sea}} - T_o}{T_o} (k^* - k) \right)^{-1} \quad (2)$$

where T_{sea} is the sea surface temperature (SST) under a storm, T_o is the TC outflow temperature determined by the atmospheric vertical profile, k^* is the saturation enthalpy of the sea surface, and k is the surface enthalpy in the TC environment.

The relationship between MPI and LMI (Equation (1)) can only be applied under limited TC conditions. For example, the relationship is invalid under the following conditions: (1) The storm moves quickly from a region with a high potential intensity to one with low potential intensity. In this case, the actual LMI can exceed the theoretical MPI because a storm needs time to adjust to its new environment. (2) The storm faces unfavorable environmental conditions, such as a strong vertical wind shear (VWS), or is influenced by the land. In this case, the actual LMI cannot approach the theoretical MPI. (3) The storm is weak. In this case, the actual LMI cannot match the theoretical MPI, given that the structure of a weak storm cannot sensitively respond to a changing environment. Therefore, by selecting only the TCs that satisfy these strict conditions, we can use the new approach to quantitatively estimate the ratio of the exchange coefficients for intense TCs (Equation (2)).

The objectives of this study are (i) to investigate the behavior of C_k/C_d as a function of wind speed, under severe winds, and (ii) to examine whether the new air-sea exchange flux parameterization based on current results can contribute to improving TC intensity prediction. We designed a numerical experiment using the state-of-the-art HWRF model to achieve the second objective and applied it to idealized and real hurricane cases. Section 2 describes the data and methods used in this study. In Section 3, we show the estimated C_k/C_d results and compare them with the findings of other methods. Section 4 shows the result of TC prediction using modified exchange coefficients in HWRF. The conclusions and discussions are provided in Section 5.

Data and methods

The LMI is estimated using the TC position and intensity obtained from the best track data of the Joint Typhoon Warning Center (JTWC) for the WNP, and the National Hurricane Center (NHC) for the NA and the ENP. For storms that achieved their LMI more than once, the actual LMI is chosen when the storm maintains its intensity for longer. Since the LMI of TCs can reach the theoretical MPI under limited conditions, we select only TCs that satisfy the following conditions: (1) The storm should have sufficient time to adjust to the new environment as it moves; i.e., the storm translation speed should not exceed 7 m s^{-1} . (2) The storm should keep quasi-steady conditions at the LMI stage; i.e., it should maintain its strength for at least 12 h after reaching the LMI. (3) The environmental conditions along the storm track should not significantly change for at least 12 h after the storm achieves its LMI. (4) The representative dynamic and thermodynamic factors related to the TC intensity, VWS, and SST should not be unfavorable for storm development. Specifically, the average VWS within a 300 km radius should be lower than 10 m s^{-1} , and the SST should be higher than 26°C . (5) The storm should have an intensity of at least Category 2 (above 40 m s^{-1}). (6) The storm should be unaffected by land; i.e., there are no landmasses within a 300 km radius of the storm center. From the 2,255 TCs that occurred in the NA, ENP, and WNP basins between 1980 and 2015, the period when the TC intensity can be accurately estimated using geostationary satellites, 84 TCs satisfied the above conditions (Table S1, Figure S2).

The MPI is calculated using Emanuel's potential intensity program ('pcmin' code) based on Equation 1, in which a scaling factor (VREDUC) of 0.8 is used to reduce the gradient wind to the surface wind. For the MPI calculation, the atmospheric input is obtained from the daily atmospheric temperature and humidity profile data from the Modern-Era Retrospective Analysis for Research and Applications (MERRA) dataset in a $1.5^\circ \times 1.5^\circ$ longitude-latitude grid. The SST under the storm (T_{sea}) is obtained from oceanic reanalysis data from the NCEP Global Ocean Data Assimilation System (GODAS), which provides pentad ocean subsurface temperatures at 40 geometric depth levels in a $1.5^\circ \times 0.333^\circ$ longitude-latitude grid for 1980 to present. The depth-averaged temperatures (T_{80}) from the surface to a depth of 80 m are calculated by averaging the GODAS data from the surface to the 80 m depth after the ocean temperature is interpolated to a 1 m depth interval. The MPI, including enthalpy (k and k^*) at the LMI location, is calculated by averaging the values within a 300 km radius of the storm center using pre-storm conditions (3 days before LMI) (Lin et al., 2013). To test the sensitivity of the SST data to the C_k/C_d calculation, we calculate additional MPIs using Group for High-Resolution Sea Surface Temperature (GHRSST) data, which are produced daily at the Canadian Meteorological

Centre with a spatial resolution of $0.2^\circ \times 0.2^\circ$. Since the GHRSST data are only from September 1991, the MPIs are derived only for the 38 TC cases that satisfy the previously described conditions from 1991 to 2015.

Numerical prediction experiments for the idealized and real TC cases are conducted using the HWRF to test the new air-sea exchange flux parameterization. This study uses the 2017 HWRF version, which has a 3 km spatial resolution. Further details regarding the input data and model setup are described in Biswas et al. (2018). The International Best Track Archive for Climate Stewardship (IBTrACS), produced by the NHC and the JTWC, is used to verify the TC forecasts (Knapp et al., 2010).

New parameterization of C_k/C_d

Figure 1A shows a scatter plot of C_k/C_d as a function of LMI, which is estimated using Equation (2) for the 84 selected TCs. The estimated C_k/C_d ranges from 0.2 to 1 for wind speeds of $40-75 \text{ m s}^{-1}$, and it clearly increases with the MWS. Based on these results, we estimate the wind dependency of the ratio using a regression function (Figure 1A) and apply this, instead of the traditionally used constant C_k/C_d (unity), to Equation 1. As a result, the correlation between the observed LMI and the theoretical MPI significantly increases from 0.34 to 0.86. The error decreases from 29.3 m s^{-1} to 5.4 m s^{-1} (refer to the blue and red dots shown in Figure 1B, respectively). Therefore, the increasing C_k/C_d with wind speed at strong winds above 40 m s^{-1} may help estimate a realistic intensity of intense TCs (this possibility is examined in the next section). A comparison of our mean C_k/C_d values (red symbol and line in Figure 2) with those in earlier studies, especially at wind speeds above 40 m s^{-1} , shows that our results are generally within the range of Bell et al. (2012) but much smaller than those of Emanuel (1995). Figure S3 shows the pre-storm SST-based C_k/C_d obtained using GHRSST and GODAS. The similar pattern between the two datasets suggests that the present method is not highly sensitive to the SST data selection and the considered analysis period.

In the original MPI method, T_{sea} is calculated using the pre-storm SST (Emanuel, 1988; Emanuel, 1995; Holland, 1997; Wang and Wu, 2004), which does not include the contribution of TC-induced SST cooling. The MPI in Figure 1 is also estimated using the pre-storm SST. A recent study suggested that pre-storm depth-averaged (averaged from the surface mixing depth down to the expected TC-induced mixing depth) ocean temperatures are more appropriate for calculating the MPI than the pre-storm SST (Lin et al., 2013). This is based on *in situ* air-deployed ocean-atmosphere measurement pairs collected during the Impact of Typhoons on the Ocean in the Pacific (ITOP) program. In particular, the depth-averaged temperature (T_{80}) from the surface to a depth of 80 m has been identified as the most appropriate index related to TC intensity under a wide

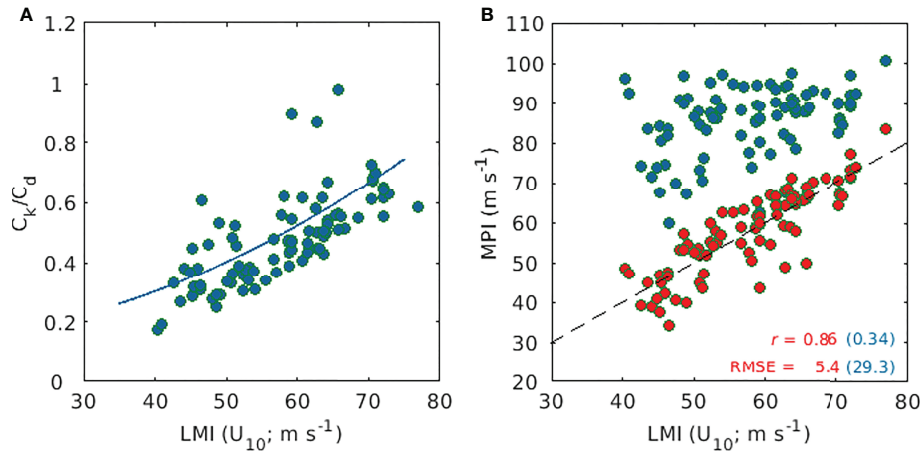


FIGURE 1

Scatter plot of C_k/C_d and theoretical MPI against LMI (i.e., MWS at 10 m, U_{10}) for major TCs. **(A)** Scatter diagram of C_k/C_d and its linear fit (blue line, $1.1013e-04 \cdot U_{10}^2 + 0.1281$) onto LMI. **(B)** Comparison of MPI calculated using unity (traditional way, blue dots) and linear fit (red dots) estimated by present approach for C_k/C_d . Correlation coefficients (r) and root mean square errors (RMSEs, $m s^{-1}$) are shown in the lower right corner.

range of major TC conditions (Price, 2009; Lin et al., 2013), although the TC-induced mixing depth also depends on the TC translation speed, size, and intensity and the upper ocean thermal structure (Price et al., 1994; Lin et al., 2009; Price, 2009).

Figure 2 compares the C_k/C_d estimated using the prestorm SST and T_{80} (blue symbol and line). The most distinct discrepancy between the two results is an overall increase in the mean C_k/C_d values and their standard deviations when T_{80} is used. This result implies that a higher C_k/C_d value is required for the storm to reach a certain intensity when the effect of storm-induced surface cooling on the MPI calculation is considered. It also suggests that numerical experiments without negative ocean feedback may lead to a different conclusion about the behavior and magnitude of C_k/C_d (Montgomery et al., 2010; Bryan, 2012; Green and Zhang, 2013; Li et al., 2016). A large increase in the standard deviation of T_{80} can be explained by the fact that the depth-averaged temperature can vary significantly due to different factors, such as the mixing depth and subsurface structure. A comparison of the two mean C_k/C_d values with those in earlier studies at wind speeds above $40 m s^{-1}$ shows that our results are generally higher than those of Bell et al. (2012) for all covered wind speeds except the $72.5 m s^{-1}$ bin, where the values are similar. At wind speeds of $40-55 m s^{-1}$, the T_{80} -based C_k/C_d regression line generally agrees with that of Soloviev et al. (2014) in terms of the positive slope of C_k/C_d (blue and dashed lines in Figure 2). However, at wind speeds above $55 m s^{-1}$, Soloviev et al.'s ratio decreases, while our calculated ratio increases with wind speed.

The continuously increasing trend of C_k/C_d at high winds is qualitatively consistent with previous results (Emanuel, 1995; Andreas, 2011; Bao et al., 2011; Bell et al., 2012; Richter and

Stern, 2014). The increasing trend of C_k/C_d at high winds is possibly due to increasing C_k (Mueller and Veron, 2014) and/or decreasing C_d (Powell et al., 2003; Jarosz et al., 2007; Vickery et al., 2009; Soloviev et al., 2014). Some previous studies attribute this tendency to the effect of sea spray (Andreas, 2011; Bao et al., 2011). As wind speed increases, the mean droplet size and the mass flux of sea spray increase. The C_k/C_d trend of continuously increasing at extreme wind speeds above $40 m s^{-1}$ may support the importance of spray-mediated air-sea enthalpy and momentum fluxes under TCs. However, the precise mechanisms responsible for this trend remain unknown.

The C_k/C_d presented here may have significant implications for improving operational TC prediction, which currently tends to underestimate major hurricanes' intensity severely. The HWRF uses C_k/C_d parameterization of the curved-fitting to available field measurements from recent observations (Biswas et al., 2018). The C_k/C_d value used in the HWRF may be too low at wind speeds above $60 m s^{-1}$. In fact, the C_k/C_d from our T_{80} -based parameterization becomes greater with increasing wind speed compared with the estimates of Soloviev et al. (2014). This suggests that using the new C_k/C_d in operational models may help reduce the negative bias in TC intensity prediction for major hurricanes, as demonstrated in the next section.

Effects of new C_k/C_d parameterization on TC intensity prediction

To examine the impact of the new parameterization of enthalpy-momentum exchange coefficients, we perform three

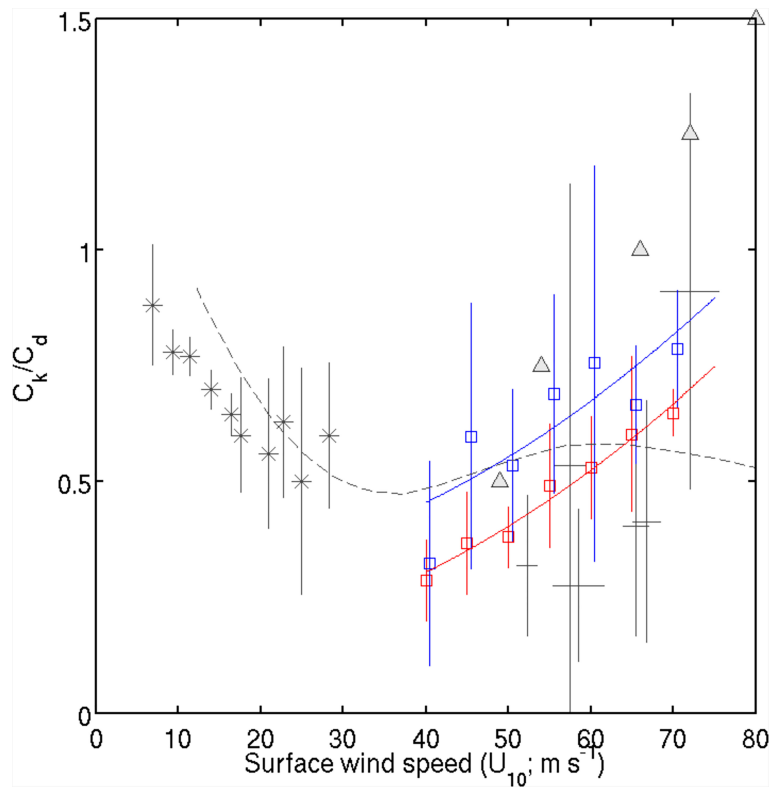


FIGURE 2

Dependence of C_k/C_d on U_{10} based on prestorm SST and depth-averaged temperatures compared with previous studies. The red and blue squares indicate the mean values of C_k/C_d within each 5 m s^{-1} interval of wind speed, estimated using prestorm SST and depth-averaged temperatures (T_{80}), respectively. The color lines and error bars indicate linear fits and one standard deviation in the bins (the linear fit of the blue line is $1.0943e-04 U_{10}^2 + 0.2799$). The dashed gray lines indicate data adapted from Soloviev et al. (2014), and the gray triangles indicate data adapted from Emanuel (1995). The mean and 95% confidence intervals of diverse laboratory and measurement results (DeCosmo et al., 1996; Zhang et al., 2008; Haus et al., 2010; Bell et al., 2012) are shown in gray asterisks and solid lines.

sets of numerical experiments using the HWRF. In the first experiment (CTRL), we use the original C_d parameterization of the HWRF (version 3.9a), in which C_d and the surface roughness lengths (z_o) level off at 50 m s^{-1} (black line in Figures 3A, B). This is based on Soloviev et al. (2014) with slight modifications (Biswas et al., 2018). The other two experiments employ the increasing C_k/C_d trend derived from our T_{80} -based parameterization. The increasing C_k/C_d ratio can mean that C_d decreases, or C_k increases, or both C_d decreases and C_k increases. It is difficult to modify both C_d and C_k simultaneously because we cannot deduce the ratio accurately, and limited computation resources are not enough to test every possible combination of C_k and C_d . Therefore, to investigate the individual impact of the coefficients on TC intensification, we employ two types of increasing C_k/C_d parameterization: 1) decreasing C_d with nearly constant C_k (C_d _DC, red line in Figures 3A, B; CTRL, black line in Figures 3C, D) and 2) increasing C_k with the original C_d (C_k _IC, blue line in Figures 3C, D; CTRL, black line in Figures 3A, B).

The effects of the modified flux parameterizations on TC simulations are investigated using three sets of experiments—CTRL, C_d _DC, and C_k _IC (Table 1)—for idealized and real TC cases, in which all experiments are identical except that different surface exchange coefficients are used. We first investigate the sensitivity of parameterization in an idealized uncoupled experiment where the atmospheric model receives no feedback from the ocean. The experiment was conducted using an idealized HWRF framework configured for the operational HWRF triple domain configuration with a grid spacing of 13.5-, 4.5-, and 1.5 km (Biswas et al., 2018). The initial intensity of the idealized vortex was 20 m s^{-1} and the radius of maximum winds was 90 km, which is embedded in a quiescent ambient. The base-state temperature and humidity profile are based on Jordan's Caribbean sounding (Gray et al., 1975). The SST is constant in time and space (304.75 K), and there is no land in the domain (Figure 4A).

Next, a series of idealized coupled TC simulations are conducted to investigate how the new C_k/C_d parameterization

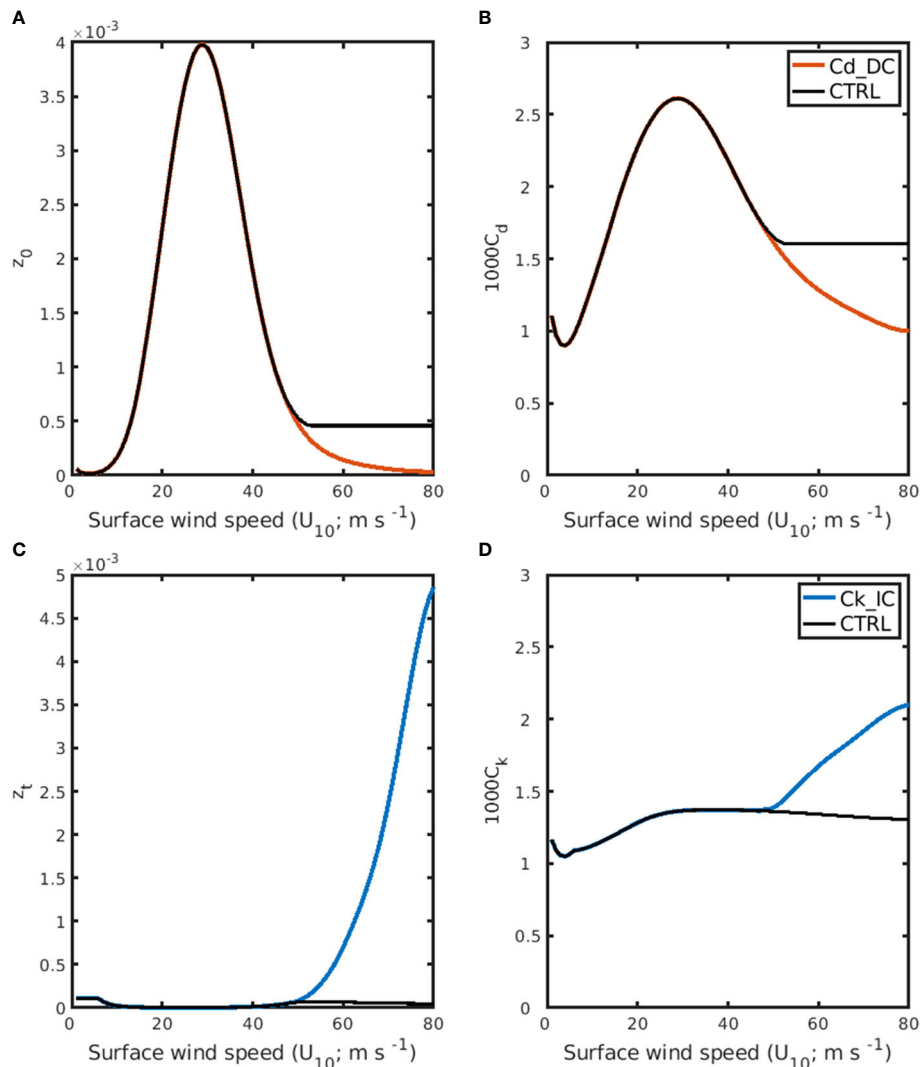


FIGURE 3

Parameterization of (A) roughness lengths for momentum z_0 , (B) drag coefficient C_d , (C) roughness lengths for heat and humidity, and (D) heat exchange coefficient C_k as a function of 10-m wind speed, as used in the CTRL, Cd_DC and Ck_IC experiments (CTRL, black curve; Cd_DC, red curve; Ck_IC, blue curve).

under high winds modulates the air-sea interactions and how it affects TC intensification. A three-dimensional ocean model, Message Passing Interface Princeton Ocean Model-Tropical Cyclone (MPIPOM-TC), is embedded into the HWRF

(HWRF-MPIPOM-TC). A coupler developed by NCEP serves as a hub for MPI communications between the HWRF atmosphere and MPIPOM-TC by which the surface fluxes and SSTs are exchanged between the HWRF atmospheric grids and

TABLE 1 Numerical experimental design to investigate the effect of air-sea flux parameterizations on TC simulations using HWRF.

Experimental Name	Air-sea flux parameterizations above 50 m s^{-1}	
	C_d	C_k
CTRL	Original HWRF (constant)	Original HWRF (nearly constant)
Cd_DC	Decreasing C_d	Original HWRF (nearly constant)
Ck_IC	Original HWRF (constant)	Increasing C_k

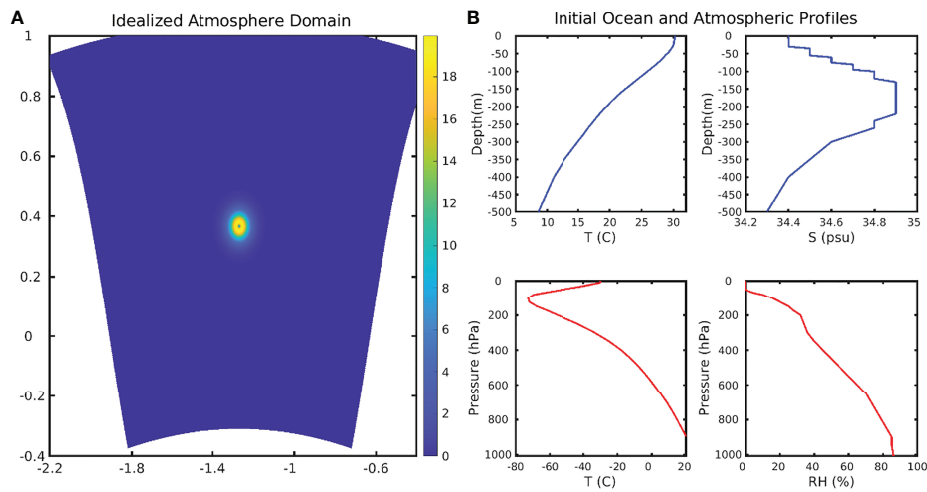


FIGURE 4

(A) Model domain for idealized experiments. Colors show wind speed with the initial vortex situated at the center of the domain. (B) Initial oceanic and atmospheric profiles used in idealized experiments. All initial temperature and salinity profiles for the ocean and initial temperature and humidity sounding are horizontally uniform.

the MPIOM-TC grids. The initial ocean fields used for this experiment are horizontally uniform and based on temperature and salinity profiles as shown in Figure 4B.

In addition to the idealized experiments, two real-case experiments for Hurricane Irma (2017) and Typhoon Mangkhut (2018) are conducted. In this experiment, as in the idealized cases, the three parameterizations in Table 1 are also tested using a coupled model. Each simulation is integrated for 126 hours, and the output is saved every three hour. As described

earlier, the three sets of experiments are identical except for using different surface exchange coefficients.

Figure 5 shows the time series of 48-h moving averaged MWS from three experiments in both idealized uncoupled and coupled experiments. Here, the TC intensity changes for the three different parameterizations have a similar trend during the first 24 h when the MWS has not yet reached 50 m s^{-1} . This is because the C_d and C_k parameterizations at wind speeds below 50 m s^{-1} are the same in all three experiments. However, after

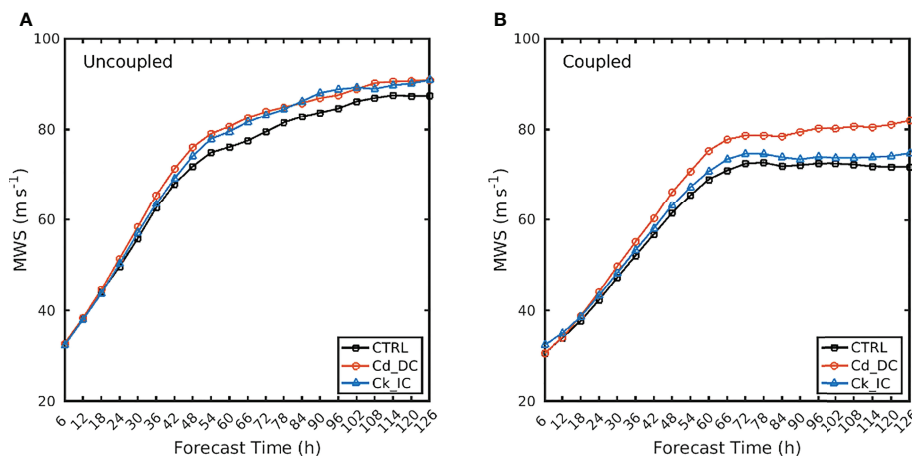


FIGURE 5

Time series of maximum wind speed (m s^{-1}) for three simulations of idealized uncoupled (A) and coupled (B) experiments. Wind speeds are smoothed by a 48-h moving average.

24 h, the Cd_DC and Ck_IC simulations persistently produce a greater MWS than the CTRL simulation. The TC intensity in the coupled model is lower in the uncoupled experiment due to the negative feedback from the ocean. Interestingly, in uncoupled simulations, the MWS in the Cd_DC and Ck_IC are similar to each other at all forecast times (Figure 5A), while, in coupled experiments, Cd_DC simulates a stronger than Ck_IC by up to 14 m s^{-1} (Figure 5B). To examine why the intensity differs between the Cd_DC and Ck_IC in coupled experiments, we conducted six idealized ensemble experiments forced with different combinations of atmospheric initial and boundary conditions and analyzed TC-induced sea surface temperature cooling (SSC) as well as air-sea humidity difference ($\Delta Q = Q_s - Q_a$). The SSC is calculated as the SST of each forecast time from 6 h to 120 h minus the SST of the initial forecast time, in which the SST is averaged within 50 km from the TC center for each forecast time.

The SSC for all three experiments tends to increase as the MWS increases. A closer look reveals that the SSC from both CTRL and Ck_IC is greater than that of Cd_DC (particularly, the difference is statistically significant above the 99% confidence level between 60 m s^{-1} and 80 m s^{-1}) (Figure 6). Because the wind stress is proportional to the C_d times the wind speed squared, a decreased C_d reduces the momentum flux into the ocean, inhibiting vertical mixing of the upper ocean. Consequently, SSC in the Cd_DC experiment is reduced, thereby increasing heat fluxes that contribute positively to TC intensification (Figure 7). Based on the bulk aerodynamic formula, increased

C_k also contributes to the increase of heat fluxes favoring for TC intensification. Both decreased C_d and increased C_k under high winds can positively contribute to the TC intensification; however, the contribution of C_d is more significant than that of C_k because C_d affects not only frictional dissipation but also the heat flux in high winds.

To investigate the effectiveness of the proposed parameterization, Cd_DC, Ck_IC, CTRL experiments are conducted for two Category 5 TCs: Hurricane Irma (Figure 8A) and Typhoon Mangkhut (Figure 8B). We forecasted 25 (15) times for Irma (Mangkhut) every 6 hours from 1200 UTC 30 August (0000 UTC 8 September) to 1200 UTC 5 September 2017 (1200 UTC 11 September 2018). The prediction results are evaluated for TC intensity (i.e., MWS) above 50 m s^{-1} with different parameterizations of the surface exchange coefficient in three experiments. Statistics show that Cd_DC outperforms both CTRL and Ck_IC in terms of the mean absolute error and bias in the intensity prediction of Irma and Mangkhut (Figure 9). For Irma, all absolute errors increase rapidly with the forecast lead time up to 48 h, but they level off thereafter. The difference between the three experiments becomes evident after 48 h, in which the error of Cd_DC is smaller by about 15% than that of CTRL after 48 h (Figure 9A). The bias differences between the experiments can mainly explain the reduction in error. That is, the negative bias of Cd_DC is smaller by 19% than that of CTRL after 48 h (Figure 9C). In contrast to Cd_DC, Ck_IC errors are slightly lower or similar to the CTRL errors. For Ck_IC, the mean absolute error after 48 h

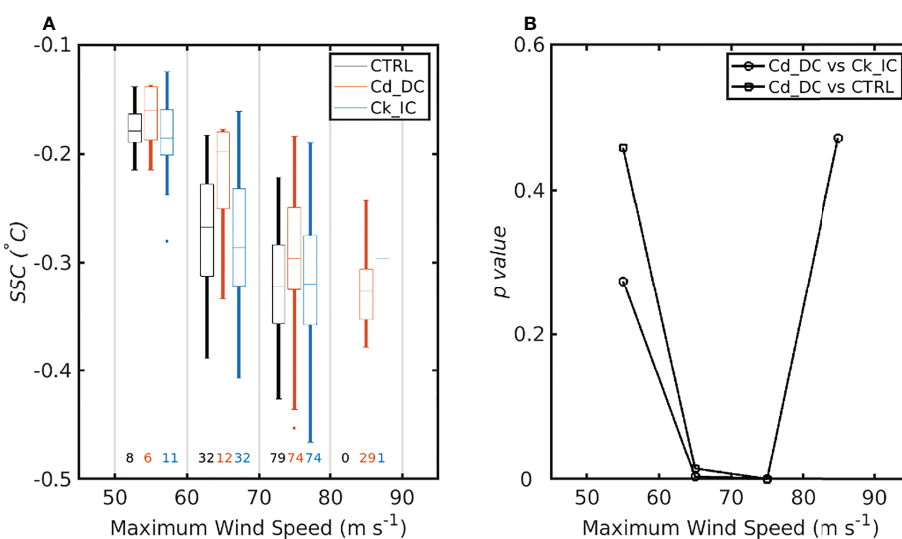


FIGURE 6

(A) Boxplots for sea surface cooling ($^{\circ}\text{C}$) as a function of MWS at each 10-m s^{-1} interval. The lines denote the median values, and the box covers the 25%-75% quartile. The bars show the minimum and maximum values, and the points show the outliers. Colors indicate results for CTRL (black), Cd_DC (red) and Ck_IC (blue). The numbers above the x-axis denote the assigned TC case number for each experiment. (B) The distribution of p -value for the SSC differences between Cd_DC and Ck_IC (solid open circle) and between Cd_DC and CTRL (solid open square). The p -values are based on Student t-test.

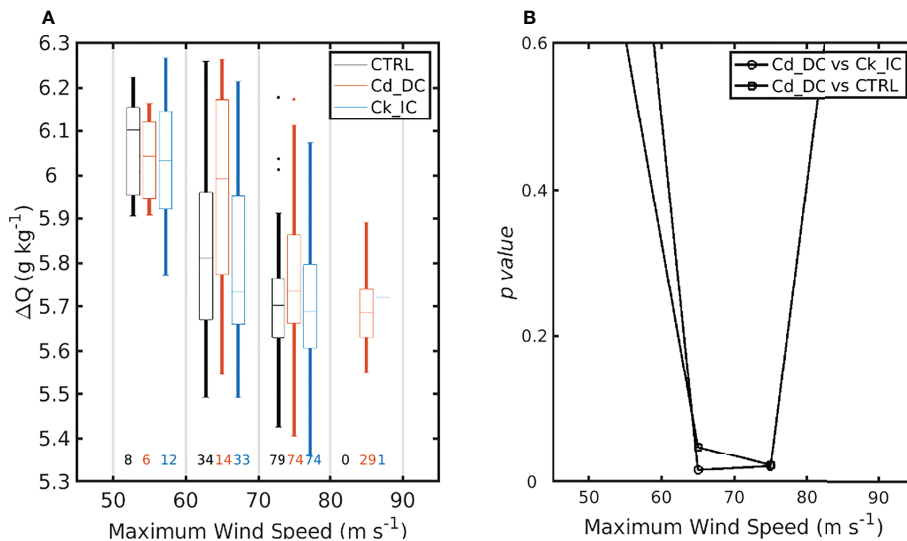


FIGURE 7

Same in Figure 6, but for (A) the air-sea moisture difference and (B) its p-values. The p in the p-values is italicization.

is reduced by about 3% compared to the CTRL. For the case of Mangkhut, the bias and errors of Cd_DC are significantly reduced at most forecast lead times (Figures 9B, D). In particular, for all forecast leads, Cd_DC reduced the absolute error on average by ~32% compared to CTRL. On the other hand, Ck_IC forecasts are not significantly improved compared to CTRL. These results are similar to those of Irma, implying that decreasing C_d can reduce the TC intensity error more effectively than increasing C_k under high winds.

In the Cd_DC experiment, the constant C_d at winds above 50 m s^{-1} is only replaced by a C_d that continues to decrease with increasing wind speed. This suggests that such improvement in intensity prediction for the two TCs is attributed to the reduction in C_d . To summarize, the decrease in C_d at high winds provided two favorable conditions for TC intensification: (1) a decrease in frictional dissipation at the air-sea interface and (2) and an increase of air-sea enthalpy (latent plus sensible heat) fluxes due to the reduced SST cooling caused by the decrease in momentum flux into the sea. Again, this emphasizes that decreasing C_d at high winds might be vital in improving intensity prediction for major TCs.

Conclusions and discussions

We present a new parameterization of C_k/C_d at high wind speeds above 40 m s^{-1} that uses the relationship between the observed LMI and theoretical MPI. This new parameterization shows that C_k/C_d increases with wind speed. We conduct triplet numerical experiments using the HWRF model, called CTRL, Cd_DC, and Ck_IC, to investigate whether the proposed

parameterization can improve TC intensity prediction. The first uses C_d that is constant at wind speeds above 50 m s^{-1} , the second uses C_d that decreases continuously with wind speed (as C_d decreases, C_k/C_d increases with wind speed due to the constant C_k used in the HWRF model) and the last uses C_k that increases continuously with wind speed (as C_k increases, C_k/C_d increases with wind speed due to the nearly constant C_d above 50 m s^{-1} used in the HWRF model). Ck_IC and Cd_DC show stronger TC intensity than CTRL in both idealized uncoupled and coupled experiments. However, there is no significant difference in TC intensity between Ck_IC and Cd_DC in the uncoupled simulations, while the intensity of Cd_DC appears to be stronger than Ck_IC in the coupled simulations. The results show that the decreased C_d not only reduces frictional dissipation but also causes a reduction in the air-sea momentum flux, consequently inhibiting SSC. The extra energy supplied by the reduced SSC in the Cd_DC experiment simulated a stronger TC than in the CK_IC experiment. Similar results are found in the numerical simulations of two category-5 TCs, Hurricane Irma (2017) and Typhoon Mangkhut (2018). Both Cd_DC and Ck_IC reduced negative bias in TC intensity prediction; however, only the former result was statistically significant. This suggests that decreasing C_d may be more effective than increasing C_k in reducing the underestimation of TC intensity in the coupled model simulation.

Efforts have been made in recent years to find the optimal parameterization of air-sea exchange coefficients on TC evolution using an atmosphere-ocean coupled modeling system (Chen et al., 2018; Liu et al., 2022). Using the atmosphere-ocean coupled experiment, Chen et al. (2018) performed a sensitivity test of three C_d parameterizations

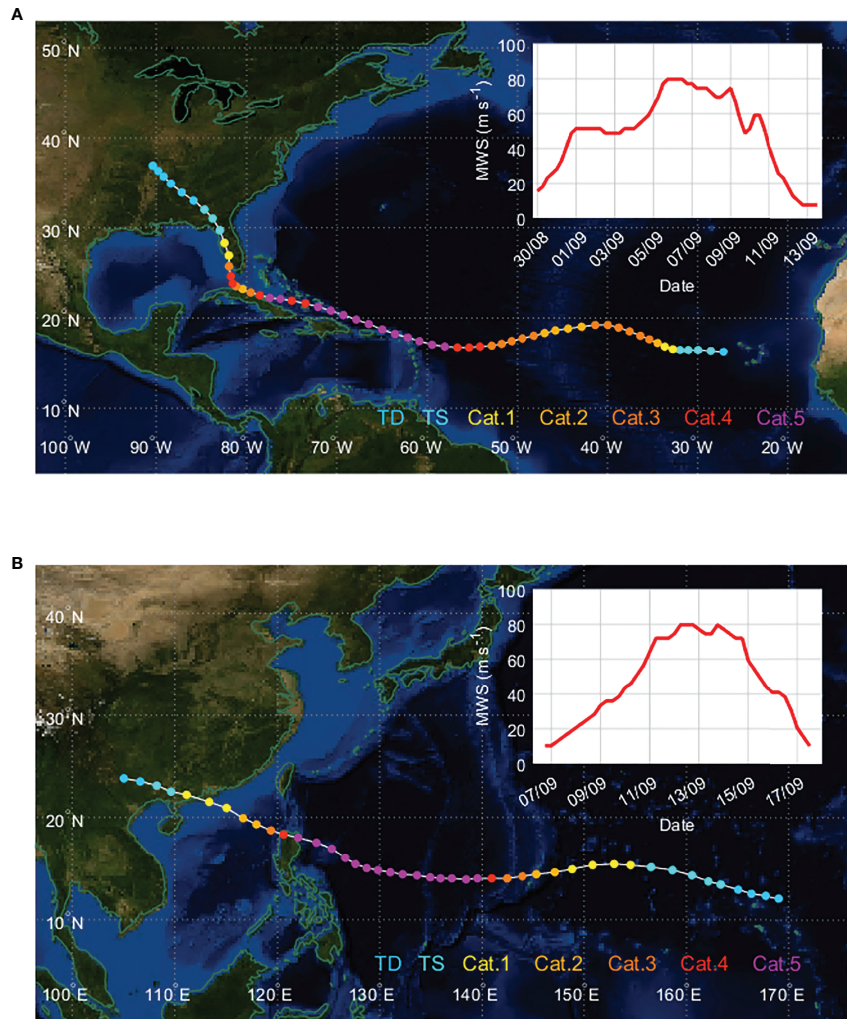


FIGURE 8

(A) Hurricane Irma over North Atlantic in 2017 and (B) Typhoon Mangkhut over the western North Pacific in 2018. The best-track positions and maximum wind speeds (in the box) are shown at 6-h intervals along with the intensity of the Saffir-Simpson wind scale (filled circle).

(increase, decrease, and level off in high winds) for Hurricane Katrina. Their study indicated that the use of a momentum flux parameterization with decreasing C_d and default C_k (Chen and Yu, 2016; C_k/C_d ratio increased) in high winds improve the accuracy of TC intensity prediction for very strong wind. Liu et al. (2022) performed sensitivity experiments of C_d parameterization using a coupled model and compared the sea surface cooling reproduced in the model with buoy data. They found that the heat flux was significantly affected by the C_d -induced sea surface cooling effect rather than the change in wind speed in the model results. Their main findings are consistent with ours regarding the importance of the use an atmosphere-ocean coupled model, resulting in better understanding of the flux exchange between TCs and the ocean.

In this study, we estimate C_k/C_d under the most intense TCs using the MPI approach, which has some limitations that need to be discussed. First, technically, the MPI defined by Equation 1 is the axisymmetric gradient wind at the top of the boundary layer, while the LMI is the maximum 1-minute sustained 10 m surface wind, which is a different metric from the MPI (Emanuel and Rotunno, 2011). This study uses a VREDUC factor of 0.8 in the MPI calculation using Emanuel's 'pcmin' code to reduce the maximum gradient wind (Vmax) to the surface wind. However, a possible scenario is that C_k/C_d is constant, but the mixing of momentum in the boundary layer changes as a function of the intensity such that VREDUC is variable instead of constant in a comparison of MPI and LMI. This is based on the relationship between C_k/C_d and Vmax, which can be affected by the

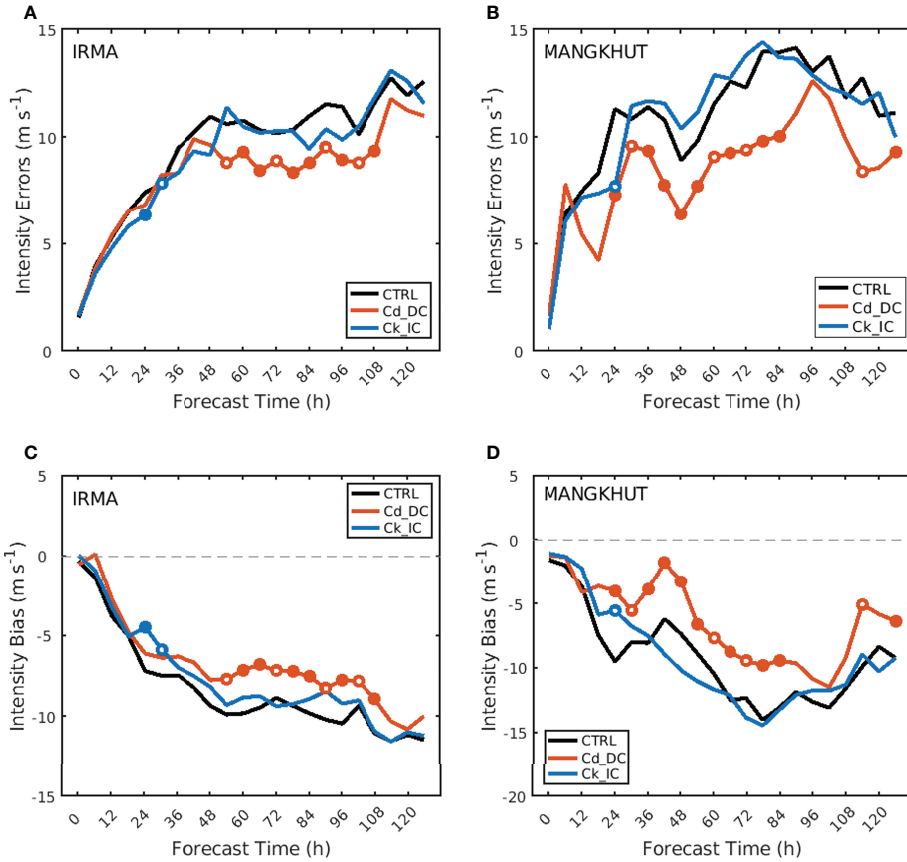


FIGURE 9

Comparisons of mean absolute error (A, B) and mean bias (C, D) against forecast lead time for three experiments, CTRL (black line), Cd_DC (red line), and Ck_IC (blue line), for Irma (A, C) and Mangkhut (B, D). Red (blue) filled [open] circles indicate that the binned value for Cd_DC (Ck_IC) is significantly improved than for CTRL at the 99% [95%] confidence level (Student's *t*-test).

parameterization of turbulence in an axisymmetric model (Bryan and Rotunno, 2009). If the identified relationship is actually between the gradient wind and surface wind as a function of wind speed, both 40 m s^{-1} and 80 m s^{-1} surface winds should have the same gradient wind as that of 80 m s^{-1} , since our regression function of C_k/C_d (blue line in Figure 2) shows ~ 0.5 at 40 m s^{-1} and ~ 1.0 at 80 m s^{-1} . This cannot happen in reality, as the TC should keep a similar magnitude of the relationship between the gradient wind at the top of the boundary layer and the surface wind.

Second, when the VREDUC factor of 0.8 reduces the gradient wind to the surface wind, the reduced values are not constant; they are a function of wind speed. The factor reduces 80 m s^{-1} to 64 m s^{-1} (16 m s^{-1} reduction) and 40 m s^{-1} to 32 m s^{-1} (8 m s^{-1} reduction, which is half the reduction at 80 m s^{-1}). Actually, the turbulence length scale in an axisymmetric model may affect the relationship between C_k/C_d and Vmax (Bryan and

Rotunno, 2009; Bryan, 2012), however not imply that the turbulence length scale is a function of wind speed. There may also be concerns about going from the axisymmetric wavenumber (0 Vmax) to the Earth-relative wind anywhere in the storm. However, we believe that the problem of going from axisymmetric to point values would be small, given that we chose only storms that moved relatively slowly. Vukicevic et al. (2014) also showed that the azimuthal wavenumber $0 + 1$ wind strongly correlates with maximum intensity (as traditionally defined), providing additional support for our approximation.

Lastly, based on theory, the k in Equation 1 is the 10 m enthalpy at the radius of maximum winds (RMW), not the ambient enthalpy. However, it is technically challenging to calculate an accurate enthalpy at the RMW because the spatial resolution ($1.5^\circ \times 1.5^\circ$) of the MERRA data used in the present analysis is not enough to resolve the eyewall and the uncertainty in the estimated RMW. Therefore, this study calculated the

enthalpy and MPI by averaging values within a 300 km radius of the storm center rather than using point values at the RMW. We also estimated the MPI using prestorm conditions (3 days before LMI) (Lin et al., 2013) to avoid modifications in the atmospheric and oceanic profiles due to air and moisture supply and oceanic mixing accompanied by TCs. A series of sensitivity experiments revealed that the averaging areas (100 km to 500 km or a donut-shaped path along the RMW) and the MPI calculation time (0 to 3 days before MPI) do not significantly affect the main results.

There are reasonably convincing studies for decreasing C_d and increasing C_k under severe wind. As wind speed increases, the ocean becomes covered by foam and C_d is reduced due to the slippery surface after the foam at the air-sea interface disappeared (Powell et al., 2003). Donelan (2018) showed that C_d decreased due to the sheltering of the surface in the lee of steep waves. Soloviev et al. (2014) suggest that C_d can also decrease because the Kelvin-Helmholtz instability at the air-sea interface leads to an absence of short surface waves (the instability grows more quickly due to large shear for short waves). It is known that sea spray is a crucial factor in the development of TCs, which are responsible for the enhancement of energy flux from the ocean to the atmosphere (Andreas and Emanuel, 2001; Andreas, 2011). Andreas (2011) projected a significant C_k increase with wind speed because of the increasing importance of spray-mediated transfer although the C_k ratio is varied with surface temperature and atmosphere stratification.

An accurate estimation of air-sea enthalpy and momentum fluxes is key to improving intensity forecast accuracy in numerical weather prediction models (Sroka and Emanuel, 2021). Whether C_k/C_d decreases or increases at extreme winds above 50 m s⁻¹ remains debatable. Limitations also exist in our method of estimating C_k/C_d . Nevertheless, this study provides important clues for understanding C_k/C_d behavior at high winds, where field observations are difficult. We also show through real TCs simulations that applying the new C_k/C_d parameterization to TC prediction can significantly reduce the negative intensity bias. However, numerical experiments and verifications in more cases are needed to generalize the present results. Our prediction results still show negative biases in high winds, suggesting that other factors, such as TC model resolutions and physics should be further improved.

Data availability statement

The original contributions presented in the study are included in the article/[Supplementary Material](#). Further inquiries can be directed to the corresponding author.

Author contributions

Conceptualization, S-HK and I-JM; methodology, WL and S-HK; validation, WL and S-HK; formal analysis, WL and S-HK; data curation, WL; writing-original draft preparation, WL; writing-review and editing, I-JM, S-HK, MB and IG; supervision, I-JM, S-HK, MB and IG. All authors contributed to the article and approved the submitted version.

Funding

This work was funded by the Korea Meteorological Administration Research and Development Program “Development of Asian Dust and Haze Monitoring and Prediction Technology” under Grant (KMA2018-00521) and Research Program funded by the Ministry of Education (2021R1A2C1005287) and the Korea government (MSIT) (RS-2022-00144325) through the National Research Foundation of Korea (NRF) and by the project titled “Study on Air-Sea Interaction and Process of Rapidly Intensifying Typhoon in the Northwestern Pacific”, funded by the Ministry of Oceans and Fisher (20220566).

Conflict of interest

The authors declare that the research was conducted in the absence of any commercial or financial relationships that could be construed as a potential conflict of interest.

Publisher's note

All claims expressed in this article are solely those of the authors and do not necessarily represent those of their affiliated organizations, or those of the publisher, the editors and the reviewers. Any product that may be evaluated in this article, or claim that may be made by its manufacturer, is not guaranteed or endorsed by the publisher.

Supplementary material

The Supplementary Material for this article can be found online at: <https://www.frontiersin.org/articles/10.3389/fmars.2022.1046511/full#supplementary-material>

References

- Andreas, E. L. (2011). Fallacies of the enthalpy transfer coefficient over the ocean in high winds. *J. Atmospheric Sci.* 68 (7), 1435–1445. doi: 10.1175/2011jas3714.1
- Andreas, E. L., and Emanuel, K. A. (2001). Effects of Sea spray on tropical cyclone intensity. *J. Atmospheric Sci.* 58(24), 3741–3751. doi: 10.1175/1520-0469(2001)058<3741:eooss>2.0.co;2
- Bao, J.-W., Fairall, C. W., Michelson, S. A., and Bianco, L. (2011). Parameterization of sea-spray impact on the air-sea momentum and heat fluxes. *Monthly Weather Rev.* 139 (12), 3781–3797. doi: 10.1175/mwr-d-11-00007.1
- Bell, M. M., Montgomery, M. T., and Emanuel, K. A. (2012). Air-Sea enthalpy and momentum exchange at major hurricane wind speeds observed during CBLAST. *J. Atmospheric Sci.* 69 (11), 3197–3222. doi: 10.1175/jas-d-11-0276.1
- Bender, M. A., and Ginis, I. (1999). Real-case simulations of hurricane-ocean interaction using a high-resolution coupled model: Effects on hurricane intensity. *Monthly Weather Rev.* 128 (4), 917–946. doi: 10.1175/1520-0493(2000)128<0917:rcsoho>2.0.co;2
- Bister, M., and Emanuel, K. A. (1998). Dissipative heating and hurricane intensity. *Meteorol. Atmospheric Phys.* 65 (3), 233–240. doi: 10.1007/BF01030791
- Biswas, M. K., Abarca, S., Bernardet, L., Ginis, I., Grell, E., Iacomo, M., et al. (2018). *Hurricane weather research and forecasting (HWRF) model: 2017 scientific documentation (Technical report)* (Boulder, CO: National Center for Atmospheric Research and Developmental Testbed Center).
- Black, P. G., D'Asaro, E. A., Sanford, T. B., Drennan, W. M., Zhang, J. A., French, J. R., et al. (2007). Air-sea exchange in hurricanes: Synthesis of observations from the coupled boundary layer air-Sea transfer experiment. *Bull. Am. Meteorol. Soc.* 88, 357–374. doi: 10.1175/BAMS-88-3-357
- Bryan, B. H. (2012). Effects of surface exchange coefficients and turbulence length scales on the intensity and structure of numerically simulated hurricanes. *Monthly Weather Rev.* 140, 1125–1143. doi: 10.1175/MWR-D-11-0023.1
- Bryan, B. H., and Rotunno, R. (2009). The maximum intensity of tropical cyclones in axisymmetric numerical model simulations. *Monthly Weather Rev.* 137, 1770–1789. doi: 10.1175/2008MWR2709.1
- Chen, Y., and Yu, X. (2016). Enhancement of wind stress evaluation method under storm conditions. *Clim Dyn* 47, 3833–3843. doi: 10.1007/s00382-016-3044-4
- Chen, Y., Zhang, F., Green, B. W., and Yu, X. (2018). Impacts of ocean cooling and reduced wind drag on hurricane Katrina, (2005) based on numerical simulations. *Monthly Weather Rev.* 146 (1), 287–306. doi: 10.1175/MWR-D-17-0170.1
- Curcic, M., and Haus, B. K. (2020). Revised estimates of ocean surface drag in strong winds. *Geophysical Res. Lett.* 47, 32020GL087647. doi: 10.1029/2020GL087647
- DeCosmo, J., Katsaros, K. B., Smith, S. D., Anderson, R. J., Oost, W. A., Bumke, K., et al. (1996). Air-sea exchange of water vapor and sensible heat: The humidity exchange over the Sea (HEXOS) results. *J. Geophysical Res.* 101, 12001–12016. doi: 10.1029/95JC03796
- DeMaria, M., Sampson, C. R., Knaff, J. A., and Musgrave, K. D. (2014). Is tropical cyclone intensity guidance improving? *Bull. Am. Meteorol. Soc.* 95, 387–398. doi: 10.1175/BAMS-D-12-00240.1
- Donelan, M. A. (2018). On the decrease of the oceanic drag coefficient in high winds. *J. Geophys. Res.-Oceans* 123, 1485–1501. doi: 10.1002/2017JC013394
- Elsberry, R. L., Chen, L., Davidson, J., Rogers, R., Wang, Y., and Wu, L. (2013). Advances in understanding and forecasting rapidly changing phenomena in tropical cyclones. *Trop. Cyclone Res. Rev.* 2, 13–24. doi: 10.6057/2013TCRR01.02
- Emanuel, K. A. (1986). An air-sea interaction theory for tropical cyclones. part I: Steady-state maintenance. *J. Atmos. Sci.* 43, 585–604. doi: 10.1175/1520-0469(1986)043<0585:AASITF>2.0.CO;2
- Emanuel, K. A. (1988). The maximum intensity of hurricanes. *J. Atmospheric Sci.* 45, 1143–1155. doi: 10.1175/1520-0469(1988)045<1143:TMIOH>2.0.CO;2
- Emanuel, K. A. (1995). Sensitivity of tropical cyclones to surface exchange coefficients and a revised steady-state model incorporating eye dynamics. *J. Atmospheric Sci.* 52, 3969–3976. doi: 10.1175/1520-0469(1995)052<3969:SOTCTS>2.0.CO;2
- Emanuel, K. A., and Rotunno, R. (2011). Self-stratification of tropical cyclone outflow. part I: Implications for storm structure. *J. Atmospheric Sci.* 68, 2236–2249. doi: 10.1175/JAS-D-10-05024.1
- French, J. R., Drennan, W. M., Zhang, J. A., and Black, P. G. (2007). Turbulent fluxes in the hurricane boundary layer. part I: Momentum flux. *J. Atmospheric Sci.* 64, 1089–1102. doi: 10.1175/JAS3887.1
- Gray, W., Ruprecht, E., and Phelps, R. (1975). Relative humidity in tropical weather systems. *Monthly Weather Rev.* 103, 685–690. doi: 10.1175/1520-0493(1975)103<0685:RHITWS>2.0.CO;2
- Green, B. W., and Zhang, E. (2013). Impacts of air-sea flux parameterizations on the intensity and structure of tropical cyclones. *Monthly Weather Rev.* 141, 2308–2324. doi: 10.1175/MWR-D-12-00274.1
- Green, B. W., and Zhang, F. (2014). Sensitivity of tropical cyclone simulations to parametric uncertainties in air-sea fluxes and implications for parameter estimation. *Monthly Weather Rev.* 142 (6), 2290–2308. doi: 10.1175/MWR-D-13-00208.1
- Haus, B. K., Jeong, D., Donelan, M. A., Zhang, J. A., and Savelyev, I. (2010). Relative rates of sea-air heat transfer and frictional drag in very high winds. *Geophysical Res. Lett.* 37, L07802. doi: 10.1029/2009GL042206
- Holland, G. J. (1997). The maximum potential intensity of tropical cyclones. *J. Atmospheric Sci.* 54, 2519–2541. doi: 10.1175/1520-0469(1997)054<2519:TMPIOT>2.0.CO;2
- Hsu, J. Y., Lien, R. C., D'Asaro, E. A., and Sanford, T. B. (2019). Scaling of drag coefficients under five tropical cyclones. *Geophysical Res. Lett.* 46, 3349–3358. doi: 10.1029/2018GL081574
- Jarosz, E., Mitchell, D. A., Wang, D. W., and Teague, W. J. (2007). Bottom-up determination of air-sea momentum exchange under a major tropical cyclone. *Science* 315, 1707–1709. doi: 10.1126/science.1136466
- Knapp, K. R., Kruk, M. C., Levinson, D. H., Diamond, H. J., and Neumann, C. J. (2010). The international best track archive for climate stewardship (IBTrACS): Unifying tropical cyclone data. *Bull. Am. Meteorol. Soc.* 91, 363–376. doi: 10.1175/2009BAMS2755.1
- Lin, I. I., Black, P., Price, J. F., Yang, C. Y., Chen, S. S., Lien, C. C., et al. (2013). An ocean coupling potential intensity index for tropical cyclones. *Geophysical Res. Lett.* 40, 1878–1882. doi: 10.1002/grl.50091
- Lin, I. I., Chen, C. H., Pun, I. F., Liu, W. T., and Wu, C. C. (2009). Warm ocean anomaly, air sea fluxes, and the rapid intensification of tropical cyclone nargis. *Geophysical Res. Lett.* 36 (3), L03817. doi: 10.1029/2008gl035815
- Li, F. N., Song, J. B., He, H. L., Li, S., Li, X., and Guan, S. D. (2016). Assessment of surface drag coefficient parametrizations based on observations and simulations using the weather research and forecasting model. *Atmospheric Oceanic Sci. Lett.* 9, 327–336. doi: 10.1080/16742834.2016.1196105
- Liu, L., Wang, G., Zhang, Z., and Wang, H. (2022). Effects of drag coefficients on surface heat flux during typhoon kalmaegi, (2014). *Adv. Atmos. Sci.* 39 (9), 1501–1518. doi: 10.1007/s00376-022-1285-1
- Montgomery, M. T., Smith, R. K., and Nguyen, S. V. (2010). Sensitivity of tropical-cyclone models to the surface drag coefficient. *Q. J. R. Meteorol. Soc.* 136 (653), 1945–1953. doi: 10.1002/qj.702
- Moon, I.-J., Ginis, I., and Hara, T. (2004). Effect of surface waves on air-sea momentum exchange. part II: Behavior of drag coefficient under tropical cyclone. *J. Atmospheric Sci.* 61 (19), 2344–2348. doi: 10.1175/1520-0469(2004)061<2344:eswoa>2.0.co;2
- Moon, I.-J., Ginis, I., Hara, T., and Thomas, B. (2007). A physics-based parameterization of air-sea momentum flux at high wind speeds and its impact on hurricane intensity predictions. *Monthly Weather Rev.* 135 (8), 2869–2878. doi: 10.1175/mwr3432.1
- Mueller, J. A., and Veron, F. (2014). Impact of sea spray on air-sea fluxes. part II: Feedback effects. *J. Phys. Oceanog.* 44 (11), 2835–2853. doi: 10.1175/jpo-d-13-0246.1
- Ooyama, K. (1969). Numerical simulation of the life cycle of tropical cyclones. *J. Atmospheric Sci.* 26 (1), 1586–1606. doi: 10.1175/1520-0469(1969)026<0003:nsotc>2.0.co;2
- Powell, M. D., Vickery, P. J., and Reinhold, T. A. (2003). Reduced drag coefficient for high wind speeds in tropical cyclones. *Nature* 422 (6929), 279–283. doi: 10.1038/nature01481
- Price, J. F. (2009). Metrics of hurricane-ocean interaction: vertically-integrated or vertically-averaged ocean temperature? *Ocean Sci.* 5 (3), 351–368. doi: 10.5194/os-5-351-2009
- Price, J. F., Sandford, T. B., and Forristall, G. Z. (1994). Forced stage response to a moving hurricane. *J. Phys. Oceanog.* 24 (2), 233–260. doi: 10.1175/1520-0485(1994)024<0233:fsrtam>2.0.co;2

- Richter, D. H., Bohac, R., and Stern, D. (2016). An assessment of the flux profile method for determining air-sea momentum and enthalpy fluxes from dropsonde data in tropical cyclones. *J. Atmospheric Sci.* 73 (7), 2665–2682. doi: 10.1175/jas-d-15-0331.1
- Richter, D. H., and Stern, D. P. (2014). Evidence of spray-mediated air-sea enthalpy flux within tropical cyclones. *Geophysical Res. Lett.* 41 (8), 2997–3003. doi: 10.1002/2014gl059746
- Richter, D. H., Wainwright, C., Stern, D. P., Bryan, G. H., and Chavas, D. (2021). Potential low bias in high-wind drag coefficient inferred from dropsonde data in hurricanes. *J. Atmospheric Sci.* 78 (7). doi: 10.1175/JAS-D-20-0390.1
- Rosenthal, S. L. (1971). The response of a tropical cyclone model to variations in boundary layer parameters, initial conditions, lateral boundary conditions, and domain size. *Monthly Weather Rev.* 99 (10), 767–777. doi: 10.1175/1520-0493(1971)099<0767:troatc>2.3.co;2
- Soloviev, A. V., Lukas, R., Donelan, M. A., Haus, B. K., and Ginis, I. (2014). The air-sea interface and surface stress under tropical cyclones. *Sci. Rep.* 4, 5306. doi: 10.1038/srep05306
- Sroka, S., and Emanuel, K. A. (2021). A review of parameterizations for enthalpy and momentum fluxes from sea spray in tropical cyclones. *J. Phys. Oceanog.* 51, 3053–3069. doi: 10.1175/JPO-D-21-0023.1
- Vickery, P. J., Wadhena, D., Powell, M. D., and Chen, Y. (2009). A hurricane boundary layer and wind field model for use in engineering applications. *J. Appl. Meteorol. Climatol.* 48, 381–405. doi: 10.1175/2008JAMC1841.1
- Vukicevic, T., Uhlhorn, E., and Reasor, P. (2014). A novel multiscale intensity metric for evaluation of tropical cyclone intensity forecasts. *J. Atmospheric Sci.* 71, 1292–1304. doi: 10.1175/JAS-D-13-0153.1
- Wang, Y., and Wu, C. C. (2004). Current understanding of tropical cyclone structure and intensity changes-a review. *Meteorol. Atmospheric Phys.* 87, 257–278. doi: 10.1007/s00703-003-0055-6
- Zhang, J. A., Black, P. G., French, J. R., and Drennan, W. M. (2008). First direct measurements of enthalpy flux in the hurricane boundary layer: The CBLAST results. *Geophysical Res. Lett.* 35, L14813. doi: 10.1029/2008GL034374
- Zhang, F., and Emanuel, K. A. (2016). On the role of surface fluxes and WISHE in tropical cyclone intensification. *J. Atmospheric Sci.* 73 (5), 2011–2019. doi: 10.1175/JAS-D-16-0011.1

Appendix

The new formulation for z_o a used in the Cd_DC experiment is

$$Z_o = \exp(p10 + p11 \times W + p12 \times W^2 + p13 \times W^3), \quad W \\ \leq 6.5 \text{ m s}^{-1}$$

$$Z_o = p25 \times W^5 + p24 \times W^4 + p23 \times W^3 + p22 \times W^2 + p21 \\ \times W + p20, \quad 6.5 \text{ m s}^{-1} \\ < W \leq 15.7 \text{ m s}^{-1}$$

$$Z_o = \exp(p35 \times W^5 + p34 \times W^4 + p33 \times W^3 + p32 \times W^2 \\ + p31 \times W + p30, \quad 15.7 \text{ m s}^{-1} \\ < W \leq 46.0 \text{ m s}^{-1}$$

$$Z_o = 10$$

$$\times \left(\frac{1}{\exp \sqrt{\frac{0.16}{p45 \times W^5 + p44 \times W^4 + p43 \times W^3 + p42 \times W^2 + p41 \times W + p40}}} \right), \quad W \\ > 46.0 \text{ m s}^{-1}$$

where W (m s^{-1}) is the wind speed, $p10 = -8.396975715683501\text{e+00}$, $p11 = -1.597898515251717\text{e+00}$, $p12 = 2.855780863283819\text{e-01}$, $p13 = -1.296521881682694\text{e-02}$, $p20 = 2.147264020369413\text{e-05}$, $p21 = 1.739759082358234\text{e-07}$, $p22 = -1.240239171056262\text{e-06}$, $p23 = 1.962282433562894\text{e-07}$, $p24 = 3.281964357650687\text{e-09}$, $p25 = 3.790846746036765\text{e-10}$, $p30 = -1.663993561652530\text{e+01}$, $p31 = 1.255457892775006\text{e+00}$, $p32 = -6.139315534216305\text{e-02}$, $p33 = 1.735308193700643\text{e-03}$, $p34 = -2.793849676757154\text{e-05}$, $p35 = 1.840430200185075\text{e-07}$, $p40 = -0.016943180834872\text{e+00}$, $p41 = 0.001980799375510\text{e+00}$, $p42 = -7.499441958611604\text{e-05}$, $p43 = 1.330088992305179\text{e-06}$, $p44 = -1.138431432537254\text{e-08}$, $p45 = 3.806734376022113\text{e-11}$